ELSEVIER

Journal of Volcanology and Geothermal Research 101 (2000) 183–198

Journal of volcanology and geothermal research

www.elsevier.nl/locate/jvolgeores

Physical models for the source of Lascar's harmonic tremor

M. Hellweg*

Institut für Geophysik, Universität Stuttgart, Stuttgart, Germany

Received 10 October 1999

Abstract

Over an 18 h interval in April 1994, the tremor at Lascar volcano, Chile, was characterized by a spectrum with narrow peaks at a fundamental freqency of about 0.63 Hz and more than 25 overtones at exact integer multiples. This harmonic tremor was recorded at four three-component, high-dynamic range stations during the deployment of the Proyecto de Investigación Sismológica de la Cordillera Occidental 94 (PISCO'94). Usually this tremor's source is modeled as the resonance of a fluid-filled crack or organ pipe-like structure in the volcano.

The resonance of a real, physical structure, however, can produce neither as many overtones nor such exact multiples as those observed in the harmonic tremor at Lascar. Harmonics also occur in a spectrum if the source signal is repetitive but nonsinusoidal. Fluid dynamics offers at least three realistic source models for harmonic tremor which produce repetitive, nonsinusoidal waveforms: the release of gas through a very small outlet (the soda bottle model), slug flow in a narrow conduit, and von Kármán vortices produced at obstacles. These models represent different flow regimes, each with its own characteristic range of Reynolds numbers. For each model the fundamental frequency of the tremor is related to the Reynolds number for the flow. Combining the Reynolds numbers for each model with typical kinematic viscosities for the possible fluids present in a volcano—magma, water, steam, air or some combination, at appropriate temperatures and pressures—provides limits on such physical parameters of the volcano as the dimensions of the flow conduit and the flow velocity of the fluid generating the tremor. If any single one of these three models is actually the process in the volcano which generates harmonic tremor, then the tremor is caused by movements of water or gases in the hydrothermal system near the volcano's surface.

Keywords: Lascar's harmonic tremor; Eddy shedding; turbulent slug flow; soda bottle model

1. Introduction

Some seismic signals generated by volcanoes look like those known from earthquake and explosion seismology. These events are probably produced by extensional or shear fractures in the volcano or by explosions. Such signals, however, represent only a small portion of the "seismic spectrum" of a volcano. More commonly, seismic signals from volcanoes appear to be generated continuously by some source within the volcano. These signals, which often vary in amplitude and frequency content, are called volcanic tremor. While the source of tremor is still poorly understood, it is present in some form at all active volcanoes and must be generated by movement or pressure fluctuations due to a physical or chemical process inside the volcano. Understanding volcanic tremor will therefore provide insights into these processes. Unfortunately, parameters derived from

* Corresponding address: 57 Overhill Road, Orinda, CA 94563, USA. Tel.: +1-925-254-0569; fax: +1-925-254-7075.

E-mail address: geo_enterprise@compuserve.com (M. Hellweg).

0377-0273/00/$ - see front matter
PII: S0377-0273(00)00163-3

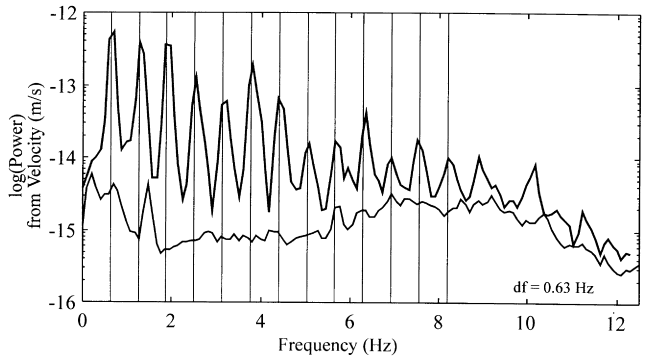

Fig. 1. Semilog power spectrum (black line) of a 10 min interval of harmonic tremor beginning at 02:35 UTC on 18.APR.94 recorded on the E component of station LA2. The spectrum was calculated using 10.24 s windows and 50% overlapping. Vertical lines are drawn at multiples of the frequency of the first peak, 0.63 Hz. The lower line is the power spectrum of a ten minute interval for the same component starting at 01:30 UTC, before the beginning of the harmonic tremor.

seismic tremor recordings can usually be related only indirectly to the variables of state in a volcano. From observations of a new type of harmonic tremor characterized by a sharply peaked spectrum consisting of a fundamental frequency and numerous integer overtones (Fig. 1) I develop new fluid dynamics models for the source of volcanic tremor. Rather than investigating the coupling of these models to the medium in detail, I concentrate on flow processes at the source.

During the deployment of a network of seismometers in northern Chile as part of the "Proyecto de Investigación Sismológica de la Cordillera Occidental '94" in early 1994 (PISCO'94, Asch et al., 1995, 1996), this unusual harmonic tremor was recorded at Lascar volcano (Fig. 2). On 18 April, for example, such tremor was recorded over an 18 h period. This continuous signal has a fundamental and many superimposed overtones. For long intervals, the frequency of the fundamental changes very little, although occasionally it rises or falls by up to 30% (Fig. 3). Regional earthquakes (arrows) have no apparent effect on the tremor's frequency. In contrast to this tremor at Lascar, harmonic signals with overtones observed at other volcanoes appear as the extended coda of volcanic events (Kamo et al., 1977; Mori et al., 1989; Schlindwein et al., 1995; Benoit and McNutt, 1997; Hagerty et al., 1997; Lees et al., 1997; Neuberg et al., 1998).

Hellweg (1999) provides a thorough analysis of Lascar's harmonic tremor using new analysis methods. She finds that this tremor's polarization offer no conclusive clues to the location of the source. At a given station the polarization direction is different for the fundamental and for each overtone. In addition, the polarization for a specific frequency, as measured at the four stations of the PISCO'94's Lascar network at any given time, cannot be reconciled with a single wavetype. Neither the amplitudes of the unfiltered nor of bandpass filtered seismograms give a coherent picture of the source. The spectral amplitudes of individual overtones at a given time appear to be uncorrelated.

The seismogram characteristic which is most consistent across components and stations is the fundamental frequency of the harmonic tremor. Hellweg (1999) demonstrates, using both phasor-walkout diagrams and plots of the reduced instantaneous phase of the Hilbert transform, that frequency changes occur at the same times and at the same rates at all stations. The frequencies of the overtones also follow the frequency of the fundamental exactly, $f_n(t) = nf_1(t)$. In some segments of the spectrograms more than 25 overtones can be observed. There are two aspects of the overtone development that are highly unusual. When resonance occurs in bodies such as organ pipes, there are seldom more than three or four harmonics present. In addition, when they exist, the theoretically calculated frequencies of higher order ($n = 25$) resonances are rarely matched precisely by measurements. In practice, the geometry of a resonator sampled by short wavelengths

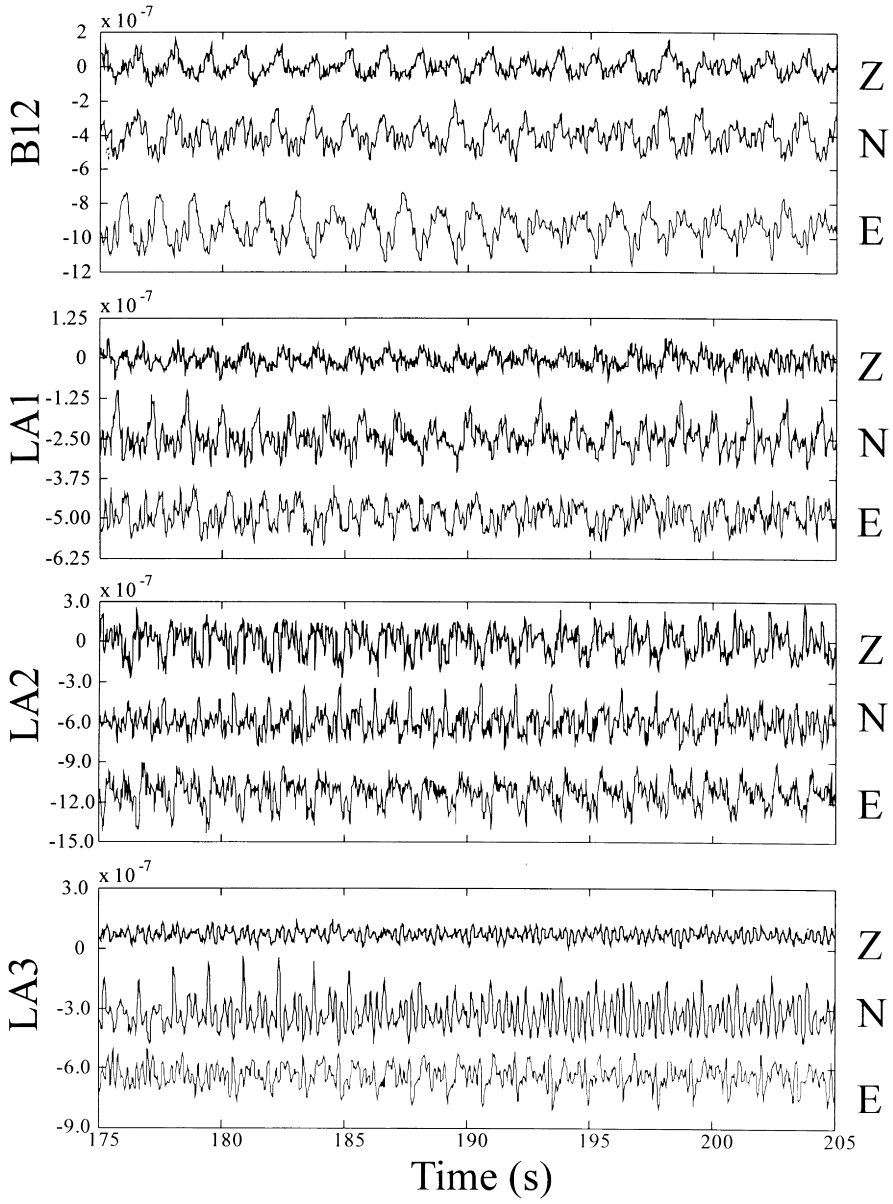

Fig. 2. Thirty seconds of harmonic tremor at all Lascar network stations. Here the broadband seismograms for station B12 are bandpass-filtered between 0.5 and 20 Hz and resampled to 50 Hz. Data for the short period stations have been lowpass-filtered and resampled to 50 Hz. The N- and E-components are offset for clarity.

corresponding to high frequencies is not the same as that sampled by the fundamental. As a result, the frequencies of the overtones are shifted slightly with respect to nf_1.

Harmonic tremor continues for several hours at a time with only small changes in the frequency of the fundamental. It appears to be a sequence of repetitions of a waveform, which changes only slowly (Fig. 2). The changes in the shape of the waveform are related to variations of the fundamental frequency, the

amplitude of the cycle, the tremor's frequency content (amplitudes of overtones) and its polarization. Since the fundamental frequency is the same at all stations, it must be a characteristic of the source. The universal presence of energy at the overtone frequencies indicates that they are also generated at or near the source.

These characteristics of harmonic tremor signals constrain the source process. The presence of numerous overtones and their exact relationship to the fundamental indicate that the source is not likely to be the resonance either of a single crack (Chouet, 1996; Benoit and McNutt, 1997; Neuberg et al., 1998) or of the gas in an organ-pipe-like structure in the volcano (Schlindwein et al., 1995; Garcés, 1997). Julian (1994) suggests that such signals are generated by non-linear flow conditions in a crack-like conduit which induce large movements of the conduit walls. The waveform generated by the source must have non-linear qualities. Thus, the source may be a non-linear vibration, such as a sound source with amplitudes that exceed the range for which the linear assumptions of acoustics are valid. It could also be a cyclic phenomenon with rapid transitions between two or more quasi-steady states (Rayleigh, 1945). Both these possibilities suggest that the source is present in the fluid phases of the volcano, rather than the solid edifice. If, for example, the source amplitudes in a solid were to exceed the range of linearity over a long time interval, the solid would eventually break or rupture. Waves generated by ruptures are well known in earthquake seismology and look nothing like harmonic tremor. Similar logic applies for the hypothesis of a cyclic source phenomenon in a solid.

Changes in the fundamental frequency of the harmonic tremor also provide clues to characteristics of the source. While they might be produced by a change in the speed of sound along the propagation path, this is unlikely to occur over an interval of seconds. Doppler shifting of a constant frequency source due to motion toward or away from the stations is can be ruled out for two reasons. The stations lie in different directions from the volcano and would therefore observe different frequency changes. Besides, the polarization remains constant for long intervals (Hellweg, 1999), indicating that the source location remains the same. Probably the frequency changes are the result of some systematic change at the source, which must be explained by the model. Models for the source of harmonic tremor must therefore be able to produce waveforms with the following characteristics:

- The signals have a well defined periodicity and steep slopes at some point during the cycle, like square or saw-tooth waves;
- the model must allow the length of the cycle to change over the time frame of minutes; and
- the process must be "non-destructive", since it continues for hours with no apparent external effect on the volcano.

2. Models

Many of the flow processes studied in fluid dynamics satisfy these criteria. They are repetitive and may continue for hours, as long as the reservoir of fluid at the source is large. There are several fluids in any active volcano that may be involved in flow processes: magma, water, either in the form of liquid or steam, and other gases such as CO_2 and SO_2. Three regimes which convert a continuous flow into pulsations that may be transmitted to the medium are eddy shedding (Faber, 1995), slug flow (Tritton, 1988) and the "soda bottle". In general, flow is described by the Reynolds number:

$$Re = \frac{ud}{\nu}. \tag{1}$$

where u is the flow velocity, d a measure of the characteristic dimension of the flow and $\nu = \eta/\rho$ is the kinematic viscosity of the fluid (its shear or dynamic viscosity divided by its density). Depending on the flow geometry, the characteristic dimension may be the cross-section of an obstruction, the diameter of the flow conduit or some other length parameter. The three models can be distinguished on the basis of the range of Reynolds numbers in which they occur. Eddy shedding occurs when the Reynolds number lies between 10^2 and 10^5 (Faber, 1995). Slug flow begins in model flow systems if the Reynolds number is about 2300 (Tritton, 1988), while the Reynolds number for the soda bottle model must be very low, on the order of 1 (Faber, 1995).

3. Eddy shedding

Eddies or vortices are a common feature of flow past bluff objects. As the flow velocity increases, the eddies are likely to detach from the object, forming a von Kármán vortex street. As each eddy develops and detaches, it imparts a force to the object and produces a sound pulse in the fluid. Because the eddies are shed regularly and with alternating vorticity, the sound pulses appear as periodic oscillations of a sound field with a characteristic frequency (Morse and Ingard, 1968). In some cases, the sound may be coupled into a feedback mechanism, producing resonance and very large sound amplitudes. As many as 10 harmonics have been observed (Morse and Ingard, 1968). Although fluid dynamics studies mainly concern themselves with the behavior of vortices behind cylinders, Hogan and Morkovin (1974) observed vortex formation at 9.5 Hz behind a 0.0013 m step when air was flowing at 3.3 m/s and Ljatkher et al. (1980) describe self-induced vibrations in a dam spillway that generate recorded amplitudes greater than 0.5 mm/s in an instrumented structure more than 2.5 km away. Vortex resonance is also associated with the formation of jets (Morse and Ingard, 1968).

When the Reynolds number is low ($Re < 10$), a fluid flows smoothly and evenly around an object. As the fluid's velocity increases, the flow separates from the object and eddies develop on its downstream side. At still higher velocities ($Re > 100$), the eddies are shed regularly, at a frequency, f_K, given by the Strouhal number:

$$St = f_K d. \tag{2}$$

For all practical purposes, $St = 0.2$ when $10^2 < Re < 10^5$ (Tritton, 1988; Faber, 1995).

For a von Kármán vortex street, the characteristic frequency, f_K, is given by Eq. (2). Taken along with Eq. (1), this equation can be solved for the flow velocity, u, in terms of frequency, the Reynolds number and the kinematic viscosity:

$$u = \sqrt{\frac{f_K \nu Re}{St}}. \tag{3}$$

Fig. 4 shows the velocity (color) for a range of Reynolds numbers and kinematic viscosities if the vortex shedding frequency is taken to be the fundamental frequency of the harmonic tremor, $f_K = f_1 = 0.63$ Hz. The Reynolds number range for which vortex resonance occurs is indicated by cross-hatching. Colored bars show typical kinematic viscosities for dry air, water and steam at one atmosphere pressure and various temperatures, for steam at 200 atmosphere pressure and for andesite melt at several temperatures (Murase and McBirney, 1973). The

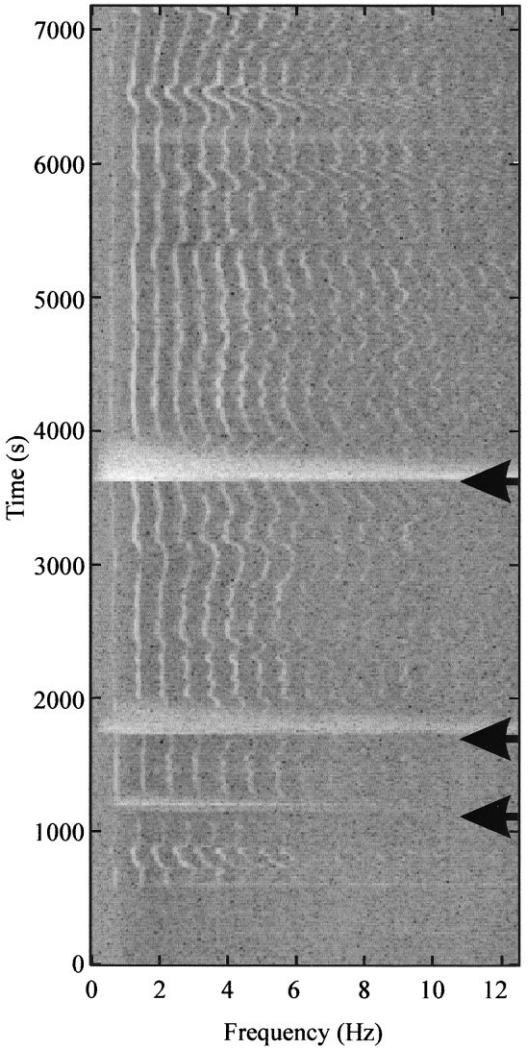

Fig. 3. Spectrogram of two hours taken from the E-component at station LA2. The data are resampled to 25 Hz. The spectrogram is calculated using data windows 10.24 s long and 50% overlapping. Arrows mark regional earthquakes.

pressure of 200 atmospheres corresponds to a depth below the surface of about 800 m. Using Eq. (2), corresponding characteristic dimensions have been calculated and are plotted as labeled, white contour lines.

If eddy shedding is the source of harmonic tremor, then Fig. 4 provides clues to the fluid involved, as well as the location and size of the obstacle causing the eddies. If, for example, the fluid is steam at high pressure, the obstacle would range in size from 4 mm to 4 cm at flow velocities of 1–10 cm/s. At the opposite end of the range of kinematic viscosity, even the most fluid andesite melt, assuming it retains the characteristics reported by Murase and McBirney (1973), must flow at 5–50 m/s through with characteristic flow dimensions of 5–50 m in order to generate vortices that would detach every $1/f_1 = 1.6$ s. On the other hand, the order of magnitude for velocity (0.1–5 m/s) and obstacle size (0.05–0.5 m) for water at 100°C, superheated steam or dry air at one atmosphere are very reasonable for sustainable activity in a volcano.

Assuming the tremor is caused by eddy shedding in a flow of steam, air or water near the volcano's surface, changes in the frequency may result from changes in the flow velocity, in the viscosity of the fluid or in the geometry of the obstacle. It is

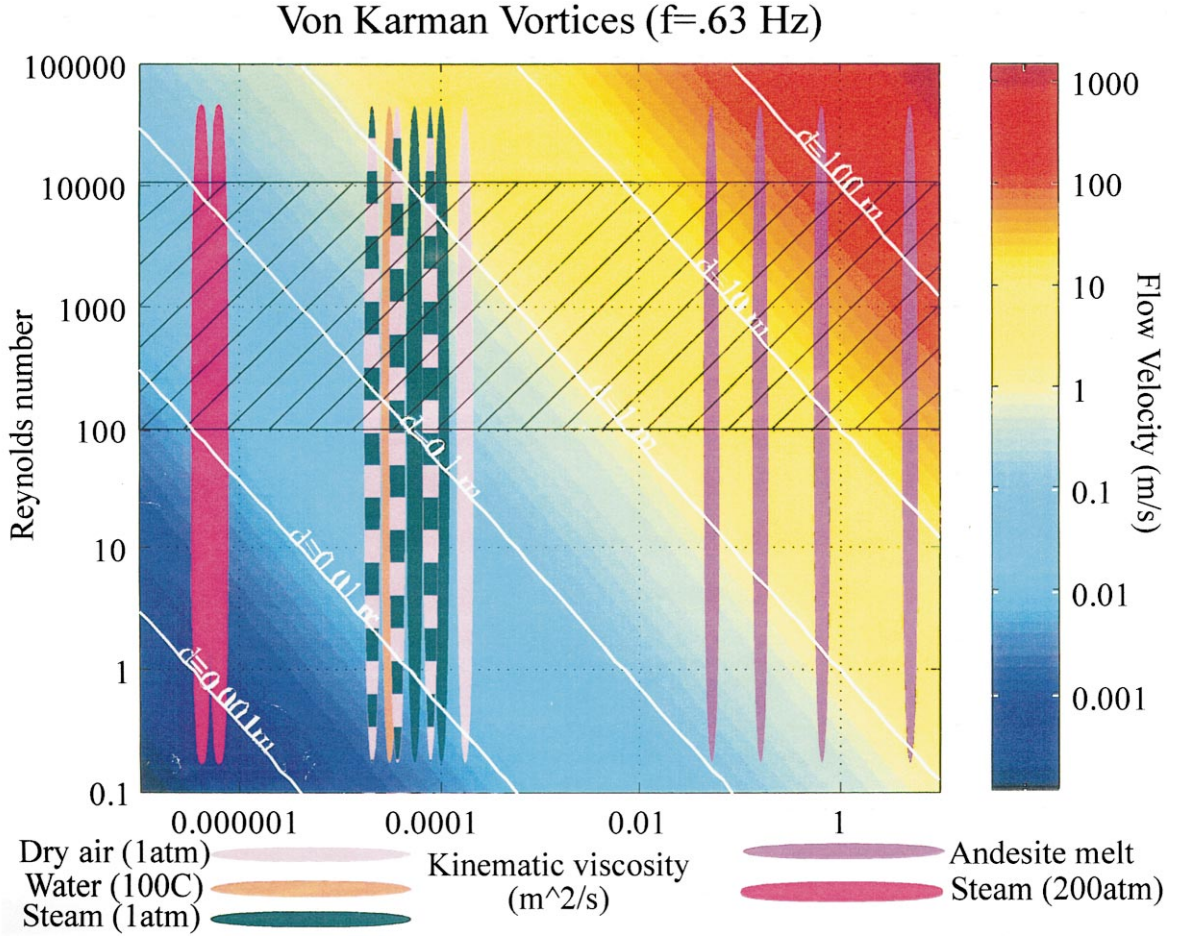

Fig. 4. Flow velocities for the eddy shedding model as a function of *Re* and kinematic viscosity when the eddy frequency 0.63 Hz. The flow velocity, denoted by color, is calculated using Eq. (3). The colored bars give typical kinematic viscosities for several fluids which may be encountered in a volcano. Eddy shedding occurs when *Re* lies within the cross-hatched region. The white lines show the flow dimension for the given constellation of kinematic viscosity and *Re*, given the eddy frequency.

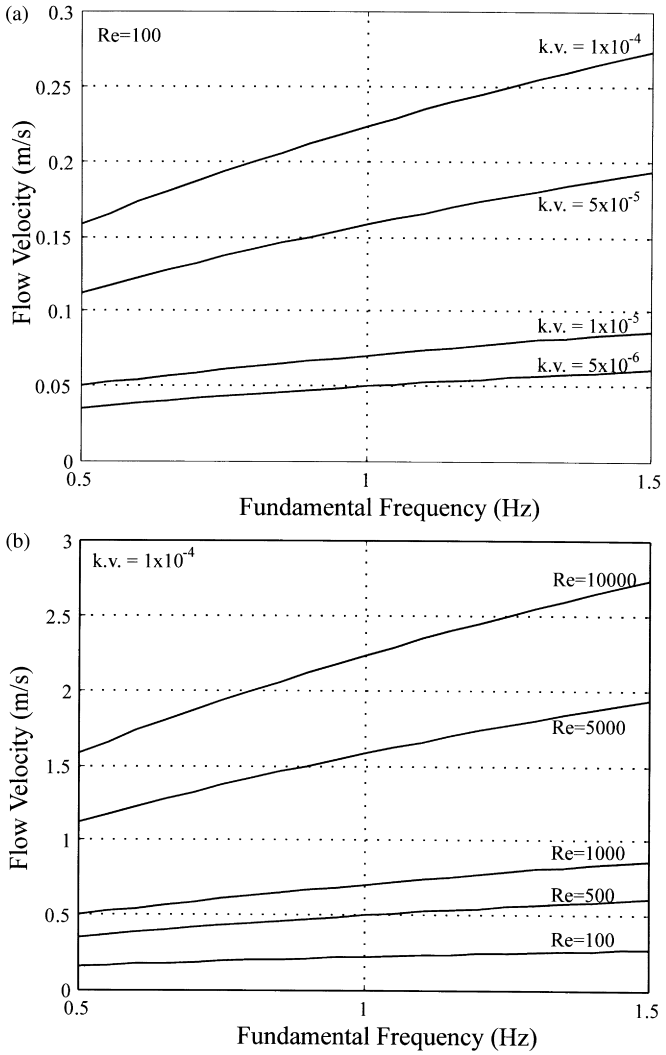

Fig. 5. Relationship of flow velocity to frequency. In (a) *Re* is held constant and flow velocities are given for various kinematic viscosities taken from the range for air, steam and water at atmospheric pressure. In (b) the kinematic viscosity is held constant and flow velocities are given as a function of shedding frequency for several values of *Re*.

improbable that the geometry of the obstacle would change rapidly and still allow the tremor to continue. Fig. 5a shows how changes in the fundamental frequency relate to changes in the flow velocity at constant Reynolds number when the kinematic viscosity changes. In Fig. 5b the relationship between flow velocity and frequency at various Reynolds numbers is shown for constant kinematic viscosity. Relatively large changes in the kinematic viscosity or the Reynolds number produce only small changes in the flow velocity and tremor frequencies. For this model, changes in the fundamental frequency on the order of 30%, as observed in Fig. 3, would be caused by changes in the flow velocity.

Shed vortices produce sound waves in two ways. First, the eddies produce density variations in the fluid, in particular when they come into contact with conduit walls, and are therefore sources of sound waves. Secondly, each time an eddy is shed from the object, it produces a force on the object.

Table 1

Fluid	Density (kg/m^3)	Velocity (m/s)	Dimension (m)	Force assuming length of 1 m (N)
Steam (2×10^7 Pa)	660	0.05	0.01	0.008
Steam (100°C)	0.6	1	0.5	0.15
Steam (400°C)	0.3	1	0.5	0.08
Water (100°C)	960	1	0.5	240
Andesite (1400°C)	2500	5	5	1.5×10^5

The force per unit length due to shedding on a cylinder of diameter d is given by Morse and Ingard (1968):

$$F_l \sim b\nu^2/2, \tag{4}$$

where b is a dimensionless constant and its range, $0.5 \leq b \leq 2$, has been determined experimentally. This force is similar to the force due to the Magnus effect. It is actually a time-varying force on the cylinder that increases as the vortex forms and reaches a maximum when the eddy is shed. In the volcano, each impulse to the obstacle as an eddy is shed will propagate in the medium as a seismic wave. For the flow velocities and dimensions given in the previous paragraph, Table 1 gives the force due to eddy shedding calculated using Eq. (4) on a cylinder of 1 m length. These values can be taken only as a rough estimate of the minimum order of magnitude for the force as they do not take resonance into account. This can intensify the force by several orders of magnitude. In addition, it is highly unlikely that the obstacle producing the eddies is a cylinder. While many papers describe observations and experimental evidence of damage due to eddy shedding, there are few measurements of the forces involved and little theory that can be applied to calculating exact forces. Blake (1986) reports that, under appropriate geometric conditions, the forces due to eddy shedding can exceed the values predicted using Eq. (4) by four orders of magnitude.

4. Turbulent slug flow

Intermittent turbulence or turbulent slugs are sometimes observed in the transition from purely laminar pipe flow to completely turbulent flow (Ginzburg, 1963; Tritton, 1988). In this case, the slug is a region of turbulence in the pipe that is separated from other turbulent segments by regions of laminar flow. The *Re* for this type of motion is calculated using the diameter of the pipe or conduit, d, as the characteristic dimension. Turbulent slugs form only if the ratio of the length of the pipe, l, to its diameter is $l/d > 50$. In addition, for a given pressure gradient, the flow rate will be higher if the flow is laminar and lower if the flow is turbulent.

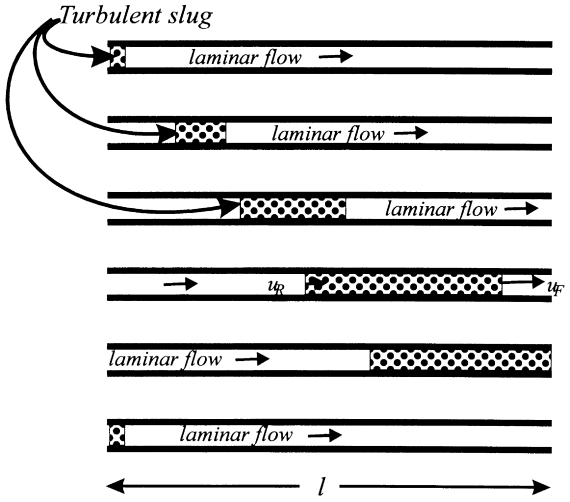

Fig. 6. Model system showing the cycle of generation of turbulence slugs. Time increases from top to bottom. Initially, laminar flow in the conduit has reached a Reynolds number at which turbulence is generated at the intake. The turbulence slows the flow and *Re* therefore decreases, so that the fluid behind the turbulent section or slug again flows laminarly. As the turbulent slug progresses through the conduit, it lengthens because its forward end progresses more rapidly than the average flow velocity while the rear end is slower. Eventually the slug leaves the end of the conduit and the flow velocity increases until a new slug is generated.

Imagine a situation, as in Fig. 6, where the flow in the pipe at a certain Reynolds number is laminar and the pressure difference between the reservoir and the outlet remains approximately constant. Experiments have shown that when the Reynolds number increases, usually due to an increase in the flow velocity, turbulence develops at the intake (Ginzburg, 1963; Tritton, 1988; Faber, 1995). Turbulence moves through the pipe at a lower velocity than the laminarly flowing fluid slowing the incoming fluid down.

Behind the turbulence, the flow becomes laminar again and the turbulent region forms a slug, which progresses through the pipe. Since its front and rear edges propagate at different velocities, the front at a higher velocity, u_F, than the "center" of the slug and the rear at a lower velocity, u_R, the slug becomes longer as it progresses. When the front end of the slug has left the pipe, the region of laminar flow behind it grows, until the rear of the turbulent slug has left the pipe. At this point, the velocity of the flow can again increase until a new turbulent slug is generated at the intake. The cycle begins again.

Propagation velocities of the front and rear of slugs have been studied experimentally. Tritton (1988, c.f. figure at p. 286) shows the ratios of u_F and u_R to the mean flow velocity u_A as a function of *Re*. Table 2 gives values of u_F/u_A and u_R/u_A for several Reynolds numbers and the corresponding intermittency factor, the fraction of time that the motion is turbulent (Tritton, 1988). At Reynolds numbers around 2300, at which turbulent slugs begin to form, u_F and u_R are very close to u_A, and slugs do not grow while flowing through the system.

The slug flow process is definitely cyclic with T_S, the period of one cycle, being determined by the length of the pipe, l, and the velocity of the rear of the slug, u_R, i.e:

$$T_S = \frac{l}{u_R}. \tag{5}$$

At the same time, the cycle can be described by the intermittency factor as:

$$T_I = \frac{T_T}{T_S} = \left(\frac{l}{u_R} - \frac{l}{u_F}\right)\left(\frac{u_R}{l}\right) = l - \left(\frac{u_R}{u_F}\right), \tag{6}$$

where T_T is the interval of turbulent flow. If, for a given configuration, the velocities of flow in turbulent and laminar regions are taken to be constant, and the change between the regions virtually instantaneous, the variation of flow velocity can be modeled as a square wave.

Table 2

Re[a]	u_R/u_A[b]	u_F/u_A[c]	Intermittancy[d]
2300			0
2500	0.88	0.96	0.08
2675	**0.87**	**1.00**	**0.13**
2750	0.85	1.05	0.19
3000	0.80	1.22	0.34
4000	0.73	1.45	0.50
5000	0.65	1.48	0.56
6000	0.60	1.48	0.59
7000	0.55	1.48	0.63

[a] Reynolds number.
[b] Relative velocity of rear of slug.
[c] Relative velocity of front of slug.
[d] Intermittancy, the fraction of the time the flow is turbulent.

For slug flow to occur in a volcano, a long narrow conduit must separate the two reservoirs of the fluid. If the volcano is not erupting and an internal reservoir is connected with the atmosphere, the fluid flowing may be water or gases. It is also possible that an appropriate conduit connects two magma reservoirs, allowing magma to flow between them. The parameters which define this model are: (1) the characteristics of the fluid; (2) the pressure difference between the reservoirs; and (3) the dimensions (length and diameter) of the connecting conduit.

The two parameters that can be measured from the harmonic tremor seismograms are: the fundamental frequency, f_1, along with the overtone frequencies and the shape of the spectrum (Fig. 1). Fig. 7 compares the power spectrum of a 10-min interval of harmonic tremor (from Fig. 1) with the power spectrum of a 13% square-wave. There is a strong correspondence between the spectra of the measured and theoretical time series, leading to the inference that the seismogram may be produced by a source function with an intermittency of 13%. The Reynolds number for flow with an intermittency of 13% is listed in Table 2.

Taking $Re \approx 2700$, Eq. (1) can be used to relate the flow velocity to the conduit size and the kinematic viscosity of the fluid (Fig. 8). Colors again denote the flow velocity. The cross-hatched area corresponds to the range of reasonable conduit sizes for a volcano, while the kinematic viscosities of andesite melt, water (100°C), steam at various temperatures and pressures, and dry air at several temperatures are marked for reference by colored bars.

Eq. (5) gives a further constraint on the geometry. If, as for harmonic tremor at Lascar, $f_1 = 0.63$ Hz, and we take $l/d = 50$, then $u_R = 50 f_1 d = 31d$. This is plotted in Fig. 8 as a white bar marked with the frequency. It gives the correspondence between

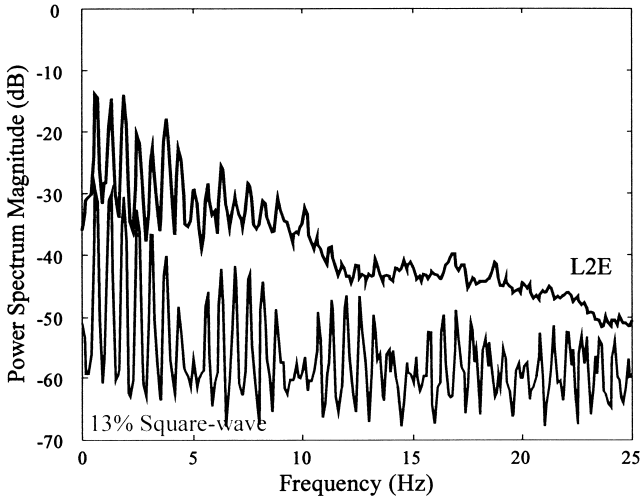

Fig. 7. Comparison between the power spectra of harmonic tremor (black, taken from Fig. 1) and a 13% square wave (lower curve).

conduit size and flow velocity, if the period of slug flow cycles is $T_S = 1.6$ s. If the kinematic viscosity of the fluid is of the order of 10^{-6} m^2/s, as it would be for steam under high pressure (about 1 km depth), the conduit would be only several centimeters in diameter, and the flow velocity would be about 0.01 m/s. Estimates for conduit size and velocity at kinematic viscosities of about 10^{-3} m^2/s, in the range for air, water and steam at various temperatures and atmospheric pressure, which would correspond to near-surface hydrothermal activity, require conduit diameters on the order of tens of centimeters and flow velocities around 1 m/s. According to this model, the flow velocity for even the least viscous andesite melt ($\sim 5 \times 10^{-2}$ m^2/s at 1400°C) is close to 100 m/s. This is highly unlikely in a volcano that is not erupting.

Thus, if the slug flow is the correct model for the source of the harmonic tremor recorded at Lascar Volcano, the source is most likely to be near the surface, and the fluid generating the signals is steam, water or gases rather than magma. Variations in the flow parameters during observations of slug flow (Tritton, 1988) should have two effects: the intermittency and the period of the cycle change as *Re* and u_R/u_F change. In a slug flow regime, the pressure at any given time and point along the conduit depends on whether the flow is mainly laminar or turbulent at that point. In a region of turbulence the pressure gradient will be steeper than where the flow is laminar, because the net movement of fluid through the conduit is less than during laminar flow (Ginzburg, 1963; Tritton, 1988; Faber, 1995).

In this model, the harmonic tremor signal measured at the stations of the Lascar network is caused by changes in the fluid's pressure which occur when the flow changes from laminar to turbulent. In principle, these pressure variations act as a variable force on the conduit walls (Wallis, 1969; Chouet et al., 1997). Practically it is difficult to estimate the relative volumes and flow velocities of laminar and turbulent fluid as a function of the cycle and it is therefore extremely difficult to estimate the amplitude of the forces on the medium during slug flow.

5. Soda bottle

When a system such as a volcano is closed to the atmosphere, the liquids, either magma or water in the hydrothermal system, must be saturated with gas. When such a system opens rapidly, as would be the case in a volcanic eruption, the rapid and explosive degassing which takes place is similar to what happens when a bottle of champagne is opened suddenly. If, on the other hand, the opening is very small, gases can only escape slowly. This may give

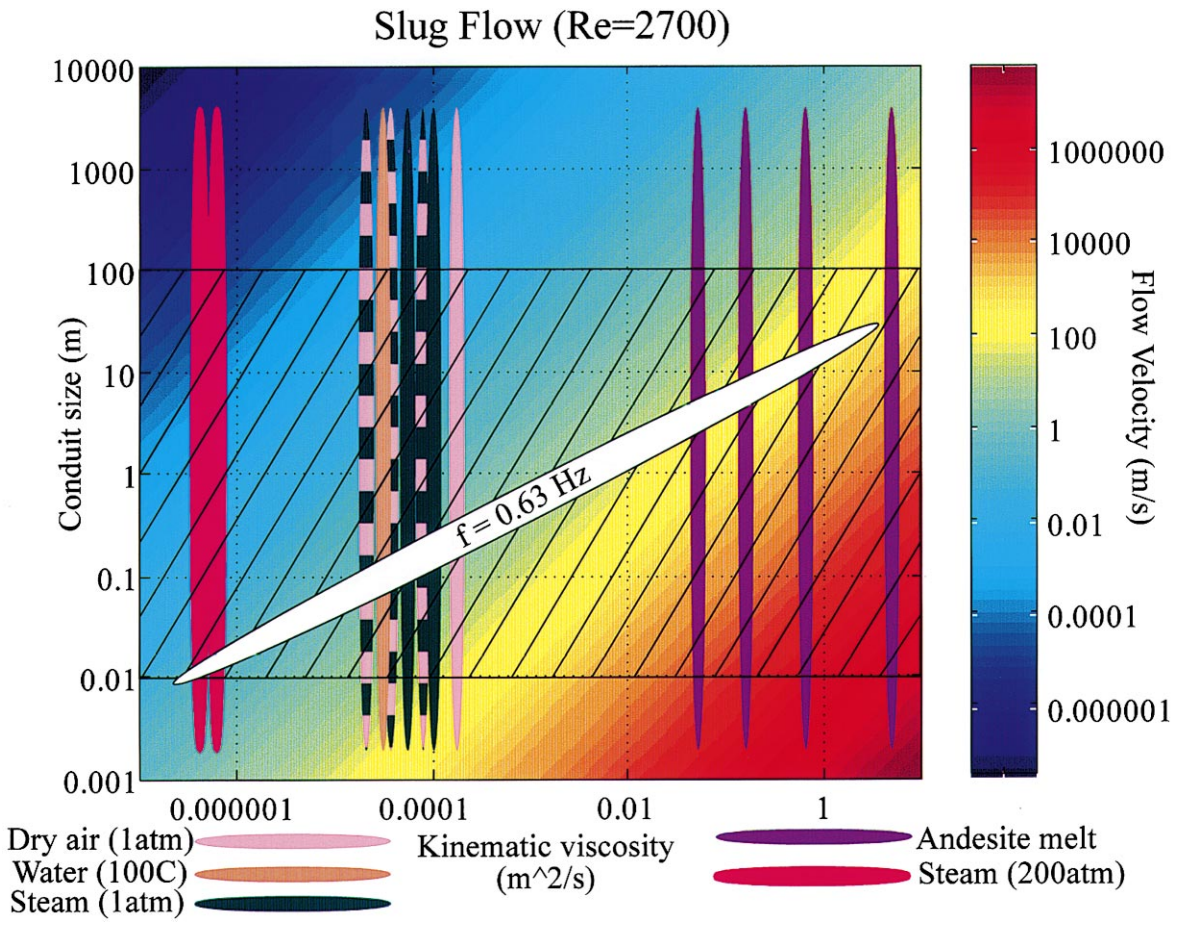

Fig. 8. Flow velocities for the slug flow model as a function of conduit size and kinematic viscosity for $Re = 2700$. The flow velocity, denoted by color, is calculated using Eq. (1). The colored bars give kinematic viscosities for fluids which may be encountered in a volcano. Conduit diameters may be reasonably expected to lie within the cross-hatched region. The diagonal white region marks configurations for which the slug flow cycle would have a period of $T = 1/f_1 = 1/0.63$ Hz.

rise to a cycle of pressure drop and bubble formation like that which can sometimes be observed when a bottle of carbonated water is opened only slightly (Soltzberg et al., 1997).

Fig. 9 shows a series of pictures taken of a bottle of soda water after its cap was opened a small amount. Initially, the gas escapes slowly with a hissing noise, and the pressure in the gas volume above the water decreases. Bubbles, which form throughout the water when the pressure has dropped enough, rise to the top during an interval depending on the size (depth) of the bottle. The volume of gas in the bubbles compensates for the pressure decrease after opening, so that shortly after the first bubbles appear, the formation of new bubbles ceases. In the meantime, gas continues to escape through the small opening or “vent” at the cap and the existing bubbles rise toward the surface. When all the bubbles have reached the surface they can no longer contribute to increase the pressure in the volume above the water, so the pressure again begins to fall as gas continues to escape. In contrast to a soda bottle, in a volcano the reservoir of gas-saturated magma or water is usually large, and may, for the purposes of a simulation, be considered to provide an infinite supply of gas allowing the tremor to continue for a long time.

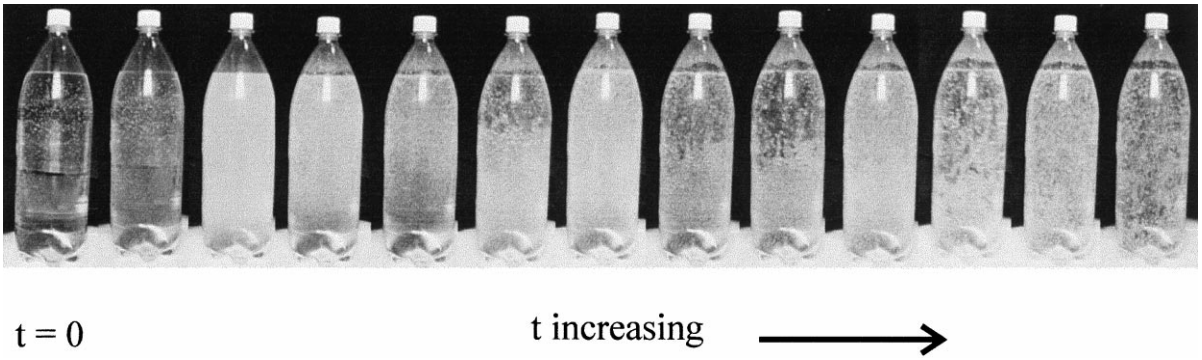

Fig. 9. Photograph sequence of two bubble cycles in a slightly opened bottle of soda water. The bottle is opened on the left, and time increases toward the right. The photographs show an interval of about 10 s.

To quantitatively describe the processes in the slightly opened soda bottle several assumptions are necessary. Fig. 10 shows sketches of a soda bottle during an interval when there are no bubbles and at a later point in the cycle when bubbles have formed, indicating the variables involved. The gas, particularly at high temperatures such as would be expected in a volcano, may be described using the ideal gas law:

$$pV = nRT = \frac{R}{M_{\text{gas}}} mT = mR'T \text{ or } p = \rho R'T \qquad (7)$$

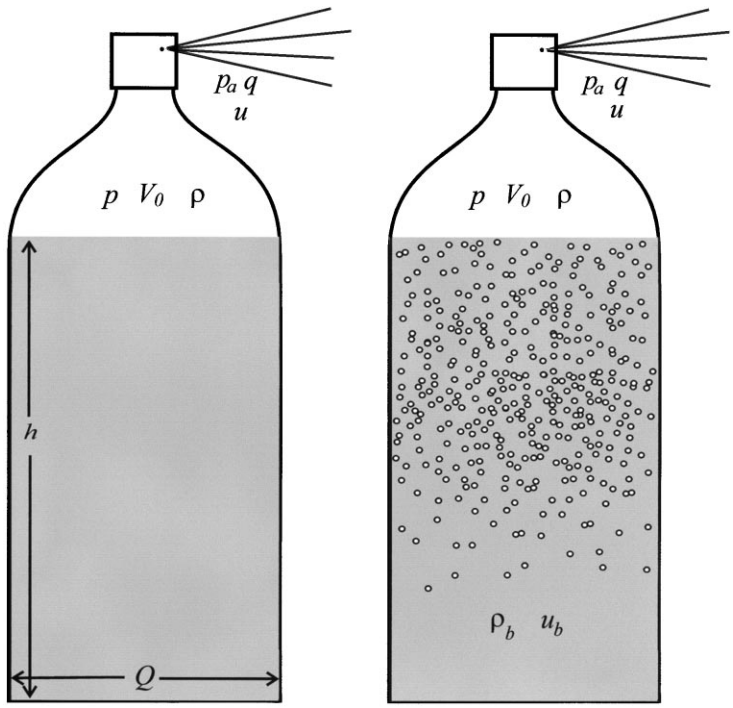

Fig. 10. Sketch of soda bottle showing parameters used in Eq. (12).

where M_{gas} is the molecular mass of the gas and $R' = R/M_{gas}$, m is the mass of gas in the volume V at the top of the bottle and ρ is its density. The mass flux may be written as:

$$R'T\dot{m} = \dot{p}V + p\dot{V}. \tag{8}$$

If we assume that the volume of the gas-filled region does not change, then $V = V_0$ and $\dot{V} = 0$. The change in pressure in the gas-filled region depends, as would be expected, on the mass flux:

$$\dot{p} = \frac{R'T}{V_0}\dot{m} = \frac{R'T}{V_0}\left[\dot{m}_e + \dot{m}_b\right] = \frac{R'T}{V_0}\left[-\rho q u + \bar{\rho}_b Q \bar{u}_b\right]. \tag{9}$$

In this equation, $\dot{m}_e$ is the mass flux due to gas escaping from the vent or cap and is the product of the density of the gas, ρ, times the cross-sectional area of the vent, q, and the velocity of the gas, u. $\dot{m}_b$ is the mass flux due to gas entering the gas-filled region from the bubbles that form in the liquid. It can be described by the mean density of the gas in the bubbles:

$$\bar{\rho}_b = n_b\left\langle \frac{4\pi}{3} r_b^3 \rho_{gas} \right\rangle, \tag{10}$$

the cross-sectional area of the liquid, Q, and the mean ascent velocity of the bubbles, $\bar{u}_b$. It is not unreasonable to assume that the geometric parameters, such as Q and q, remain constant over several degassing cycles in either a soda bottle or a volcano. Further, we may assume that the velocity of the escaping gas, u, is proportional to the difference in pressure between the interior of the bottle or volcano and the outside (Ginzburg, 1963):

$$u = k(p - p_a). \tag{11}$$

Inserting these values into Eq. (8) and using Eq. (6) for the density of the gas gives a non-linear differential equation for the pressure:

$$\dot{p} = -\frac{qk'}{V_0}p(p - p_a) + \frac{R'TQ}{V_0}\bar{\rho}_b\bar{u}_b = -\frac{qk'}{V_0}p^2 + \frac{qk'p_a}{V_0}p + c_b = -c_1p^2 + c_2p + c_b. \tag{12}$$

where $c_1 = qk'/V_0$ and $c_2 = c_1p_a$ are constants for the soda bottle, and may vary slowly as a function of time in a volcano. The final constant:

$$c_b = \frac{R'TQ}{V_0}\bar{\rho}_b\bar{u}_b, \tag{13}$$

is zero if no bubbles are present. If the bubbles rise with constant velocity, c_b may be related to the kinematic viscosity of the liquid by setting Stoke's law equal to the bubbles' buoyancy and solving for the velocity:

$$c_b = \frac{R'TQ}{V_0}\bar{\rho}_b\frac{2\pi r^2 g}{9\nu}. \tag{14}$$

Thus, it is inversely proportional to the kinematic viscosity of the liquid and depends, in addition, on the bubbles' density, their rise velocity, and the geometry of the chamber.

Eq. (12) must be solved numerically for two cases. When no bubbles are present, $c_b = 0$, and the gas pressure drops. c_b becomes a non-zero constant which controls the rate of pressure increase when bubbles are present. Fig. 11 shows solutions for several different initial conditions in a soda bottle. As c_b increases, that is with decreasing kinematic viscosity, the bubbles rise more quickly and the amplitude of the pressure oscillations increases dramatically. To produce the oscillations observed at Lascar, with a fundamental frequency of 0.63 Hz, the liquid which is degassing must have a low viscosity, and is most likely to be water near the surface at relatively low overpressure. Soltzberg et al. (1997) approach this problem differently, using different assumptions. Quantitatively, however, their results also confirm the cyclic degassing behavior demonstrated here.

Although this description of the soda bottle phenomenon is highly simplified, the model generates non-linear waveforms (Fig. 11) which bear a

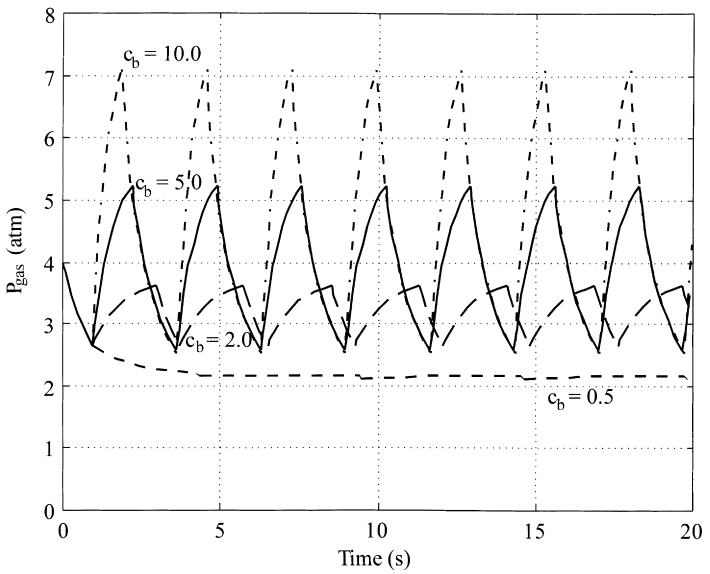

Fig. 11. Pressure oscillations in a soda bottle with a small vent. The curves' initial conditions are marked. For $c_b = 5$ and $c_b = 10$, the maximum pressure overshoots the original pressure.

resemblance to the seismograms of harmonic tremor at Lascar. They are produced by pressure variations inside the reservoir during the bubble formation cycle. Under the simple assumptions used for solving Eq. (12), the pressure changed by more than a factor of 2.0.

Achenbach (1975) gives a relationship describing the wavefield generated by pressure changes in a spherical cavity of radius A in a homgeneous, isotropic and linearly elastic medium. If the pressure change is a step function, $P(t) = P_0 H(t)$ with $H(t)$ the Heaviside function, then the displacement potential is:

$$\dot{u}_r(r,t) = -\frac{1}{4\mu}\frac{A^3 P_0}{r} \times [1 - (2-2\sigma)^{1/2}\exp(-\chi s)\sin(\varphi s + \lambda)]H(s) \quad (15)$$

where α is the speed of longitudinal waves in the medium, σ is the Poisson's ratio, μ is the shear modulus, and χ, φ and λ are defined as:

$$\chi = \frac{1-2\sigma}{1-\sigma}\frac{\alpha}{A},\ \varphi^2 = \frac{1-2\sigma}{(1-\sigma)^2}\frac{\alpha^2}{A^2},$$

$$\lambda = \cot^{-1}(1-2\sigma)^{1/2}\ (\pi/4 \le \lambda \le \pi/2),$$

and

$$s = t - \frac{r-a}{c_L}.$$

A pulse of finite duration, t, can be simulated by

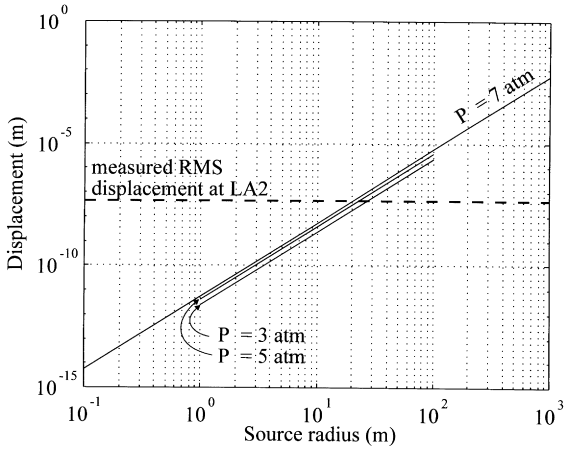

Fig. 12. Displacement amplitude due to a pressure pulse at 4000 m distance in a spherical cavity of radius a in a homgeneous, isotropic and linearly elastic medium calculated using Eq. (14). The dashed line is the root mean square displacement amplitude measured at station LA2. The solid lines are for pressure differences between the interior of the sphere and the environment of 3, 5 and 7 atm.

superimposing the displacement potential for a pressure change of equal but opposite magnitude a time τ after the initial pressurization. Using $r =$ 4000 m, $\alpha = 1000$ m/s, $\sigma = 0.3$ and $\mu = 2 \times 10^{10}$N/m^2, Fig. 12 plots the expected displacement as a function of the source radius, A, for $P_0 = 3$, 5 and 7 atm, the pressures used in the calculations for Fig. 11. The root mean square displacement measured at LA2 is also plotted as a dashed line. It intersects the lines for all three pressures at a radius of about 20 m. This indicates that, under the simplifying assumptions used here, fluctuating pressure of the order of magnitude described above in a sphere with a radius of 20 m could produce the harmonic tremor seismograms measured at Lascar.

6. Conclusions

Observations of harmonic tremor such as that recorded at Lascar Volcano in April, 1994 are still relatively rare. Nonetheless, because the source models usually used to explain tremor generation (Seidl et al., 1981; Ferrick et al., 1982; Mori et al., 1989; Julian, 1994; Schlindwein et al., 1995; Chouet, 1996) do not fit this type of tremor, it offers new insights into how volcanoes work.

The three, new, physical models for the source of harmonic tremor presented here, eddy shedding, slug flow and the soda bottle, relate observed characteristics of the tremor, in particular its fundamental frequency and the shape of the power spectrum, to fluid dynamic variables of the models such as characteristic flow dimension (i.e. conduit size), kinematic viscosity of the fluid and flow velocity. All three models give the same striking result: if the flow dimensions and velocities are to remain within reasonable bounds, then:

(1) harmonic tremor must be produced by the *movement of water or gases*, not magma;

(2) harmonic tremor must be generated *near the surface*, at close to atmospheric pressure, therefore probably in the active crater; and

(3) changes in the tremor frequency are caused by *small, easily reversible changes in flow velocity*, rather than by changes in the geometry of the volcano's conduit system.

The physical processes described by these three models occur in specific regimes of flow as described by the Reynolds number. If *Re* is lower or higher, as it would be during other flow regimes, the same flow geometry will generate other types of signals. The sound associated with turbulent flow systems, for example, is broadband noise (Tritton, 1988; Faber, 1995). Thus, these models may be applicable at most volcanoes and may, in addition, explain the continuous "background" tremor as part of the same phenomenon.

Is one of these models more realistic than the others? The period and amplitude for each model depend on a trade-off between flow geometry and velocity as well as the viscosity of the fluid involved. As is indicated by Figs. 4 and 8, a suite of these three parameters can generate the same frequency. Perhaps with further investigation of the coupling between the source and medium, an aspect of harmonic tremor recordings addressed only minimally in this description, the models can be distinguished.

Acknowledgements

PISCO'94 was part of the Collaborative Research Programme (SFB) 267, "*Deformation Processes in the Andes*". Sponsored by the Deutsche Forschungsgemeinschaft, the SFB is based at the Freie Universität Berlin (Sprecherhochschule) in cooperation with the Technische Universität Berlin, the GeoForschungsZentrum Potsdam and the Universität Potsdam. The author particularly thanks Günter Asch, who supplied the data, and Alex Rudloff and Frank Gräber, without whose efforts no data would have been collected.

References

Achenbach, J.D., 1975. Wave Propagation in Elastic Solids. Elsevier, New York, 425 pp.

Asch, G., Bock, G., Gräber, F., Haberland, C., Hellweg, M., Kind, R., Rudloff, A., Wyllagalla, K., 1995. Passive Seismologie im Rahmen von PISCO'94. In: Giese, P. (Ed.), Sonderforschungsbereich 267 Deformationsprozesse in den Anden. Berichtband für die Jahre 1993–1995. Berlin, pp. 619–677.

Asch, G., Wylegalla, K., Hellweg, M., Seidl, D., Rademacher, H., 1996. Observations of rapid-fire event tremor at Lascar volcano, Chile. Ann. Geofis. 39, 273–282.

Benoit, J., McNutt, S.R., 1997. New constraints on source processes

of volcanic tremor at Arenal volcano, Costa Rica, using broadband seismic data. Geophys. Res. Lett. 24, 449–452.

Blake, W.K., 1986. Mechanics of Flow-Induced Sound and Vibration, 1. Academic Press, New York, 425 pp.

Chouet, B., 1996. New methods and future trends in seismological volcano monitoring. In: Scarpa, Tilling (Eds.). Monitoring and Mitigation of Volcano Hazards. Springer, Heidelberg, pp. 23–97.

Chouet, B., Saccorotti, G., Martini, M., Dawson, P., De Luca, G., Milana, G., Scarpa, R., 1997. Source and path effects in the wave fields of tremor and explosions at Stromboli volcano, Italy. J. Geophys. Res. 102, 15 129–15 150.

Faber, T.E., 1995. Fluid Dynamics for Physicists. Cambridge University Press, Cambridge, 440 pp.

Ferrick, M.G., Qamar, A., St. Lawrence, W.F., 1982. Source mechanism of volcanic tremor. J. Geophys. Res. 87, 8675–8683.

Garcés, M.A., 1997. On the volcanic waveguide. J. Geophys Res. 102, 22 547–22 564.

Ginzburg, I.P., 1963. Applied Fluid Dynamics. National Science Foundation, Washington, DC, 258 pp.

Hagerty, M.T., Schwartz, S.Y., Protti, J., Garcés, M., Dixon, T., 1997. Observations at Costa Rican volcano offer clues to causes of eruptions. EOS Trans. AGU 78 (49), 565–570.

Hellweg, M., 1999. Listening carefully: unique observations of harmonic tremor at Lascar volcano, Chile. Ann. Geofis. 42, 451–464.

Hogan, J.M., Morkovin, M.V., 1974. On the response of separated pockets to modulations of the free stream. In: Naschauer, E. (Ed.), Flow Induced Structural Vibrations. Springer, Heidelberg, pp. 47–56.

Julian, B.R., 1994. Volcanic tremor: nonlinear excitation by fluid flow. J. Geophys. Res. 99, 11 859–11 877.

Kamo, K., Furuzawa, T., Akamatsu, J., 1977. Some natures of volcanic micro-tremors at the Sakura-Jima volcano. Bull. Volcanol. Soc. Jpn. 22, 41–59.

Lees, J.J., Johnson, J., Gordeev, E., Batereau, K., Ozerov, A., 1997. Volcanic explosions at Karymsky: a broadband experiment around the cone. EOS Trans. AGU 78 (46), F430.

Ljatkher, V.M., Sladnev, M.V., Sheinin, I.S., 1980. Hydroelasticity effects in hydraulic engineering practice. In: Naschauer, E., Rockwell, D. (Eds.), Practical Experiences with Flow-Induced Vibrations. Springer, Heidelberg, pp. 414–427.

Mori, J., Patia, H., McKee, C., Itikarai, I., Lowenstein, P., de Saint Ours, P., Talai, B., 1989. Seismicity associated with eruptive activity at Langila Volcano, Papua New Guinea. J. Volcanol Geotherm. Res. 38, 243–255.

Morse, P.M., Ingard, K.U., 1968. Theoretical Acoustics. McGraw-Hill. New York, 927 pp.

Murase, T., McBirney, A.R., 1973. Properties of some common igneous rocks and their melts at high temperatures. Geol. Soc. Am. Bull. 84, 3563–3592.

Neuberg, J., Baptie, B., Luckett, R., Stewart, R., 1998. Results from the broadband seismic network on Montserrat. Geophys. Res. Lett. 25, 3661–3664.

Rayleigh, J.W.S., 1945. The Theory of Sound, II. Dover, New York, 504 pp.

Schlindwein, V., Wassermann, J., Scherbaum, F., 1995. Spectral analysis of harmonic tremor signals at Mt. Semeru volcano, Indonesia. Geophys. Res. Lett. 22, 1685–1688.

Seidl, D., Schick, R., Riuscetti, M., 1981. Volcanic tremors at Etna: a model for hydraulic origin. Bull. Volcanol. 44, 43–56.

Soltzberg, L.J., Bowers, P.G., Hofstetter, C., 1997. A computer model for soda bottle oscillations: the bottelator. J. Chem. Ed. 74, 711–714.

Tritton, D.J., 1988. Physical Fluid Dynamics. Clarendon Press, Oxford, 519 pp.

Wallis, G.B., 1969. One-dimensional Two-phase Flow. McGraw-Hill, New York, 408 pp.